

# Conjugate Heat Transfer From a Vertical Plate With Discrete Heat Sources Under Natural Convection

S. Lee

Research Assistant Professor.

M. M. Yovanovich

Professor.  
Fellow ASME

Microelectronics Heat Transfer Laboratory,  
Department of Mechanical Engineering,  
University of Waterloo,  
Waterloo, Ontario, Canada

*A quasi-analytical conjugate heat transfer model is developed for a two dimensional vertical flat plate with discrete heat sources of arbitrary size and power level under natural convection. The plate is located in an extensive, quiescent fluid which is maintained at uniform temperature. The model consists of an approximate analytical boundary layer solution and a one dimensional numerical conduction analysis in which an allowance is made to account for radiation heat transfer. These fluid and solid solutions are coupled through an iterative procedure. A conjugate problem is solved when a converged temperature distribution is obtained at the plate-fluid interface, concurrently satisfying the thermal fields on both sides of the interface. Comparisons of the surface temperature variations obtained by using the present model are made with existing numerical and experimental data which were obtained for cases with two strip heat sources mounted flush with the surface of a vertical plate in air. The model is shown to be in good agreement. In addition, the convection and radiation heat flux variations are presented. The results illustrate the importance of radiation heat transfer for estimating surface temperatures of the plate.*

## Introduction

The performance level of microelectronic devices has been improving in the last few decades with such progress, that today's technological achievements in most areas could not possibly have been realized without the use of these devices. In efforts to obtain these improvements, which lead to greater input power and higher packing densities, thermal engineers are constantly faced with problems of heat dissipation. The operating temperature of a semiconductor has to be maintained below the maximum allowable temperature as specified by various design constraints, in order to ensure reliable performance of integrated circuits and to maintain low failure rates of components.

Heat transfer phenomena associated with printed circuit boards (PCBs) usually include all three modes of heat transfer, namely heat conduction through the board, heat convection into the ambient fluid and surface radiation to the surroundings. It is important, therefore, to predict heat transfer characteristics due to a simultaneous interaction between all anticipated modes of thermal energy transport.

A complete thermal modeling of a PCB is extremely complex. A detailed prediction of the thermal characteristics of a proposed PCB with a high degree of accuracy is seldom economically feasible nor technically necessary in most situations. From an economic and development point of view, a model may be used at the early stage of a board design to examine the criteria set by not only the thermal constraints but also the electrical and packaging constraints. This model may

be a simple and approximate representation of the PCB and is subject to frequent modifications and major changes without consuming great time and expense. It is to this end that the model presented herein was developed.

A PCB is often simplified as a flat plate in many analytical and numerical studies as a limiting approximation to non-smooth component carrying PCBs. In such studies, components are assumed to be mounted flush with the surface of the circuit board and, hence, the boundary layer flow experiences a flat surface at the plate-fluid interface. In the range of parameters associated with the typical PCB applications under natural convection cooling, the boundary layer flow is often laminar over the entire surface of the board. The flat plate assumption is shown to yield acceptable results that can be applied to the non-smooth component carrying PCBs (Bar-Cohen, 1985). The trend toward thinner components, and commercially growing surface mount technology, which allows components to be mounted closer to the surface of the board, are also in favor of the flat plate assumption.

The study of natural convection heat transfer from a vertical flat plate with various thermal conditions prescribed in either heat flux or temperature variations at the surface has been carried out by numerous investigators using different techniques and methods over the past several decades. It is clear, however, that the results obtained from such studies can not be utilized directly in predicting the local heat transfer characteristics of a PCB, since the thermal conditions at the surface of the actual board are arbitrary and unknown *a priori*. Besides, determination of the thermal conditions at the surface of the circuit board is often the objective in many ap-

Contributed by the Electrical and Electronics Packaging Division for publication in the JOURNAL OF ELECTRONIC PACKAGING. Manuscript received by the Electronics Packaging Division April 6, 1989.

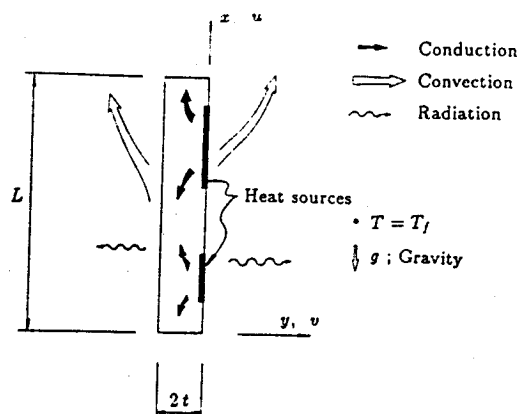
plications, which requires a conjugate analysis that simultaneously accounts for the effects of all modes of heat transfer including radiation.

Despite ubiquity of conjugate heat transfer phenomena, conjugate problems, involving natural convection from an isolated vertical plate with discrete heat sources, have not received much investigation to date. Zinnes (1969) solved two dimensional problems in air by using finite difference methods with an iterative technique to satisfy the matching of heat flux at the plate-fluid interface. He presented wall temperature variations for a vertical plate which contained up to three strip heat sources on one side with the other side insulated. He also provided experimental data which agree well with his numerical results. Further conjugate problems have been studied by Kishinami and Seki (1983), and Kishinami *et al.* (1987) using both numerical and experimental methods, but the isothermal conditions imposed over the heating sections of the plate made their results unsuitable for applications to PCBs considered herein.

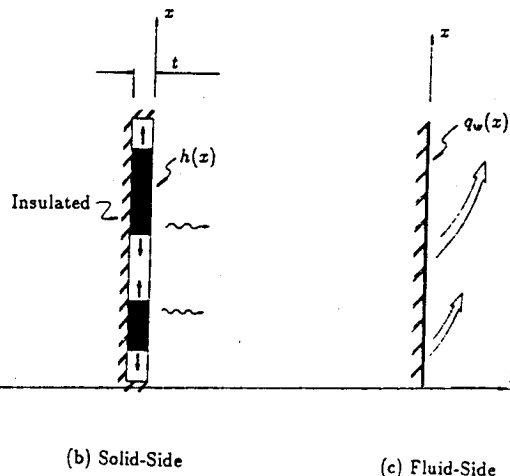
An analytical solution for the conjugate problems that are expected in thermal modeling of PCBs is not available in the literature. In this paper, a quasi-analytical model for two dimensional conjugate heat transfer from a vertical flat plate with discrete heat sources of arbitrary size and power level is presented. The fluid-side of the problem will be solved based on a new approximate analytical method developed recently by Lee (1988) for a vertical flat plate with arbitrary surface heat flux variations under laminar natural convection. The sources are assumed flush mounted such that the fluid-side convection model can be used in conjunction with a solid-side conduction model which is developed based on a simple one dimensional energy balance on a discretized domain. The fluid-side model yields a wall temperature variation given an arbitrary heat flux distribution at the surface, and the solid-side model yields a heat flux distribution convected into the fluid given an arbitrary variation of the convection heat transfer coefficient along the surface. Radiation heat transfer to the surroundings is also accounted for in the solid-side model, and solutions to the conjugate problem are obtained when thermal conditions at the fluid-solid interface are converged through an iterative procedure.

### Problem Statement

The conjugate problem under present consideration is depicted in Fig. 1(a), which shows an isolated vertical plate with a number of strip heat sources of negligible thickness imbedded flush with the surface. The plate is suspended in a quiescent fluid which is, in turn, contained within surround-



(a) Conjugate Problem



(b) Solid-Side

(c) Fluid-Side

Fig. 1 Thermal dissipation from heat sources

ings of large extent. The fluid and the surroundings are maintained at uniform temperatures of  $T_f$  and  $T_\infty$ , respectively. The plate has dimensions of thickness  $2t$ , length  $L$  parallel to the gravity vector  $g$ , and large transverse width so as to result in a two dimensional problem. The coordinates parallel and perpendicular to the plate are  $x$  and  $y$ , respectively, and corresponding components of the fluid velocity are denoted by  $u$  and  $v$ .

Heat generation within a package is normally not uniform but concentrated near the center of the package where an in-

### Nomenclature

$C$  = parameter defined by equation (6)  
 $g$  = gravitational acceleration  
 $h$  = convection heat transfer coefficient  
 $k$  = thermal conductivity  
 $L$  = length of plate  
 $N$  = total number of elements  
 $q$  = local heat flux  
 $q_w^*$  = dimensionless heat flux,  $q_w L / (T_w - T_f) k_f$   
 $Q$  = rate of heat transfer  
 $t$  = half thickness of plate  
 $T$  = temperature, absolute  
 $u$  = local velocity parallel to plate, in  $x$ -direction

$v$  = local velocity normal to plate, in  $y$ -direction  
 $x$  = vertical coordinate measured from leading edge  
 $y$  = horizontal coordinate measured from plate surface

### Greek Symbols

$\alpha$  = thermal diffusivity of fluid,  $k_f / (\rho c_p)$   
 $\beta$  = thermal expansion coefficient,  $-(\partial \rho / \partial T)_p / \rho$   
 $\gamma$  = function used in equation (5)  
 $\epsilon$  = surface emissivity  
 $\nu$  = kinematic viscosity,  $\mu / \rho$   
 $\bar{\Phi}$  = function used in equation (5)

### Subscripts

$c$  = conduction  
 $f$  = fluid conditions  
 $i$  = parameters at  $i$ -th element  
 $p$  = source conditions  
 $r$  = radiation  
 $s$  = solid conditions  
 $w$  = surface conditions  
 $\infty$  = surrounding conditions

### Dimensionless Groups

$Bi$  = Biot number,  $ht/k_s$   
 $Gr_x^*$  = modified Grashof number,  $g \beta q_w x^4 / k_f \nu^2$   
 $Pr$  = Prandtl number,  $\nu / \alpha$

egrated circuit is located. Since the information regarding internal heat generation and the material property of the package is not of the issue here, heat generated within each source will be assumed to be uniform over the volume of the package, although the present model is not limited to this condition. The sensitivity of the surface temperature variation with respect to changes in the specified heat flux profiles over a source has been examined by Culham and Yovanovich (1987) who conducted a parametric study of a simplified model of PCBs on which a uniform convection heat transfer coefficient is specified. With the negligible thickness of heat sources, the magnitude of the rate of heat generation may be given in terms of an equivalent heat flux. This heat flux will be constant over each heat source in the present study, but may differ from one source to another.

An analytical solution to the above problem does not exist. Given a conjugate problem, it may be approached by decoupling the problem into two distinct problems; one for the solid-side and the other for the fluid-side, for which solutions may be found independently by imposing assumed thermal boundary conditions at the fluid-solid interface. The solid-side model deals with conduction heat transfer in the solid, where thermal radiation to the surroundings is included. The fluid-side model deals with convection heat transfer. The coupling of convection, conduction and radiation heat transfer may then proceed by iteratively solving these two models until a convergence in the interfacial conditions is obtained to within a specified tolerance.

Further simplifications pertaining to the solid-side model can be made as follows. Firstly, if the plate is thin and the heat sources are located away from the immediate vicinity of the edges of the plate, as they usually are, heat dissipation through the edge surfaces represents a negligible amount of the total dissipation. The edges of the plate are, thus, assumed to be insulated.

Secondly, when the Biot number,  $Bi$ , based on the plate half thickness,  $t$ , is small, the temperature difference across the thickness of the plate may be neglected. A two-dimensional conjugate modeling of vertical plates under forced convection cooling indicates that this value of  $Bi$  at the center of the heat sources needs to be less than about 0.05, if the through-plane conduction is to be neglected without significantly altering the final solutions (Culham, 1988). The study found that, if a one dimensional conduction analysis is used for cases where the Biot number is 0.05, the resulting conjugate model may introduce differences up to  $\pm 5$  percent in the prediction of the maximum surface temperature excess.

The coefficient  $h$  associated with natural convection heat transfer from typical PCBs in applications ranges from approximately 5 to 20  $W/m^2K$  when air is used as the coolant fluid (Chu and Simons, 1984). If a plate with a thickness,  $2t$ , of 3 mm is considered, the above criterion permits the use of a one dimensional solid-side model in the present study for cases with the thermal conductivity,  $k_s$ , as low as 0.6  $W/mK$ . Considering this combination being one of the worst cases, it can be seen that the solid-side of the present conjugate problem can be sufficiently modeled by using a one dimensional conduction analysis for most situations. A further investigation on this subject can be found in the study of Fast *et al.* (1987).

The one dimensional approximation in the solid-side model allows the entire problem to become symmetrical about the mid-plane of the plate along the center line of the thickness. Consequently, only one half of the plate thickness needs to be considered, and half of the total heat generated by the sources will be included hereafter. The simplified solid-side problem is depicted in Fig. 1(b). The back surface, the leading and trailing edges are insulated. A variation of the convection heat transfer coefficient as a function of  $x$  is prescribed along the front surface where radiation heat transfer is taking place, simultaneously.

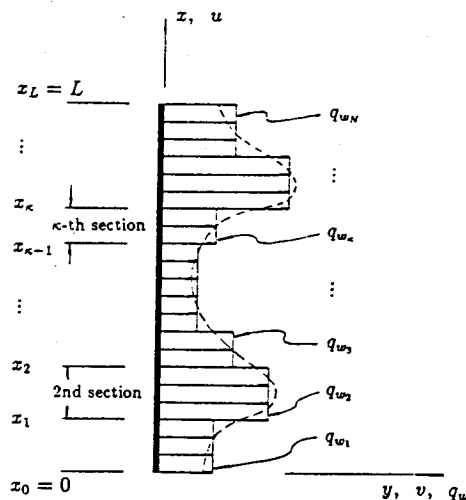


Fig. 2 Geometric configuration of fluid-side modeling shown with a step change representation of a surface heat flux variation

The fluid-side problem is depicted in Fig. 1(c), which again considers only one surface of the plate. As indicated in the figure, an arbitrary variation in convective heat flux as a function of  $x$  is specified as the surface boundary condition.

In the following, the fluid and solid-side models will be presented, and the coupling of the models will be described in detail.

### Fluid-Side Model

An approximate analytical model developed by Lee (1988) will be used as the fluid-side model. This model is capable of predicting temperature and velocity distributions across the boundary layer when a multi-step change in heat flux of an arbitrary pattern is prescribed at the plate surface.

A continuous surface heat flux variation, that can be expected from a typical conjugate problem of current interest, is drawn in Fig. 2 by a dotted line. The plate is discretized into a number of sections and the heat flux within each section is replaced by a uniform heat flux that approximately represents an average heat flux over the section. The resulting variation is a multi-step change as shown in the figure. Only a few step changes are shown here for illustration purposes. A further discretization into smaller step sizes, of course, would allow the step change approximation to closely represent the continuous variation, and then, the model can be applied. A summary of the fluid-side model is presented as follows.

The usual set of boundary layer equations that governs two dimensional, steady state momentum and energy transport in natural convection is written below.

$$u \frac{\partial u}{\partial x} + v \frac{\partial u}{\partial y} = 0 \quad (1)$$

$$u \frac{\partial u}{\partial x} + v \frac{\partial u}{\partial y} = \nu \frac{\partial^2 u}{\partial y^2} + g\beta(T - T_f) \quad (2)$$

$$u \frac{\partial T}{\partial x} + v \frac{\partial T}{\partial y} = \alpha \frac{\partial^2 T}{\partial y^2} \quad (3)$$

The boundary conditions associated with the above equations are

$$\begin{aligned} \text{at } y=0, \quad u=v=0, \quad -k_f \frac{\partial T}{\partial y} = q_{w_i} \text{ for } x_{i-1} < x \leq x_i \\ \text{as } y \rightarrow \infty, \quad u=0, \quad T=T_f \\ \text{at } x=0, \quad u=0, \quad T=T_f \end{aligned} \quad (4)$$

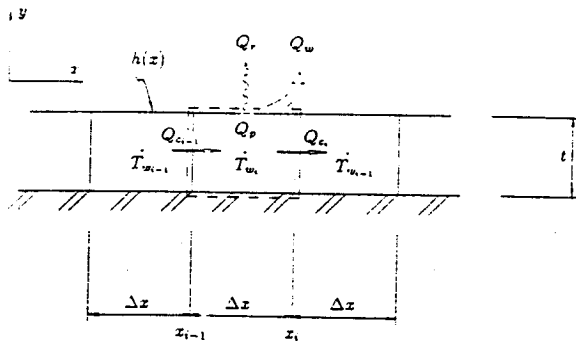


Fig. 3 Geometric configuration of solid-side modeling shown with uniformly discretized elements

where  $T$  is the local temperature,  $T_f$  is the ambient fluid temperature,  $k_f$  is the fluid thermal conductivity,  $q_{w_i}$  is the uniform surface heat flux prescribed in the  $i$ -th section for  $x_{i-1} < x \leq x_i$ , and  $x_0 = 0$ . In the above set of equations, all fluid properties, except the density variation in the buoyancy term of the momentum equation, are assumed to be constant. The dynamic pressure work and viscous dissipation terms are neglected.

A combined use of linearization of the above governing differential equations in conjunction with the integral method results in an approximate solution for the wall temperature variation in the  $\kappa$ -th section as

$$T_w = T_f + \frac{x}{k_f(C Gr_x^*)^{1/5}} \sqrt{\bar{\Phi}_\kappa} \sum_{i=1}^{\kappa} (q_{w_i} - q_{w_{i-1}}) \gamma_i \quad (5)$$

where  $q_{w_0} = 0$  and  $\bar{\Phi}_1 = \gamma_1 = 1$ .  $\bar{\Phi}_\kappa$  and  $\gamma_i$ , for  $i = 2$  to  $\kappa$ , are functions of  $\gamma_{i-1}$ ,  $q_{w_i}$ ,  $x_{i-1}$ ,  $x$  and  $Pr$ . These functions are dimensionless and can be determined by solving numerically a pair of equations which consist of a first order ordinary differential equation for  $\gamma_i$  and an algebraic equation for  $\bar{\Phi}_\kappa$ . A full description of the equations is given by Lee and Yovanovich (1989), and will not be presented here for brevity.

The value of  $C$  appearing in equation (5), is dependent only on the Prandtl number. It may be evaluated based on the correlation equation developed by Fujii and Fujii (1976) for a vertical plate with uniform surface heat flux as follows:

$$C = \frac{Pr^2}{4 + 9\sqrt{Pr} + 10Pr} \quad (6)$$

### Solid-Side Model

In this section, the one dimensional solid-side model is described. The model is developed based on an energy balance over a discretized control volume, and the differential terms associated with conduction heat transfer in the plate are replaced with the usual form of a finite difference representation. The model accounts for convection heat transfer at the surface by incorporating a convection heat transfer coefficient,  $h$ . Allowances are made to include surface radiation heat transfer to surroundings.

Figure 3 shows a section of the plate which is discretized into a total of  $N$  elements along the length. For simplicity, the elements are chosen to be of the same size. A control volume, representing the  $i$ -th element between  $x = x_{i-1}$  and  $x_i$ , is shown with the participating heat transfer terms. As was previously discussed, the present one dimensional model no longer distinguishes the actual location of heat sources within the control volume, and the rate of heat generated within the element is indicated by  $Q_p$  in the figure. Readers are reminded that  $Q_p$  represents only half of the original total heat generation since the problem was assumed to be symmetrical as described earlier.

Assuming a unit depth, conservation of energy for the  $i$ -th element results in

$$Q_p = (Q_{c_i} - Q_{c_{i-1}}) + Q_w + Q_r \quad (7)$$

where

$$Q_p = q_{p_i} \Delta x \quad (8)$$

$$Q_{c_i} = -k_s t \left. \frac{dT_w}{dx} \right|_{x=x_i} \approx -k_s t \frac{T_{w_{i+1}} - T_{w_i}}{\Delta x} \quad (9)$$

$$Q_w = q_{w_i} \Delta x = \int_{x_{i-1}}^{x_i} h(T_w - T_f) dx \approx h_i(T_{w_i} - T_f) \Delta x \quad (10)$$

$$Q_r = q_{r_i} \Delta x = \int_{x_{i-1}}^{x_i} \epsilon \sigma (T_w^4 - T_\infty^4) dx \approx \epsilon \sigma (T_{w_i}^4 - T_\infty^4) \Delta x \quad (11)$$

Here,  $q_{p_i}$  denotes the rate of heat generation per unit surface area,  $q_{w_i}$  and  $q_{r_i}$  denote the average convective and radiative heat fluxes over the surface of the  $i$ -th element, respectively. An element over non-source regions can be simply identified by letting  $q_p = 0$ . The insulated conditions at the leading and trailing edges can be implemented by setting  $Q_{c_0} = 0$  and  $Q_{c_N} = 0$ , respectively.

Given a problem with  $h_i$  specified for  $i = 1$  to  $N$ , equation (7) combined with equations (8) through (11) would result in a set of  $N$  non-linear equations for the discrete temperature distribution  $T_{w_i}$ . An iterative procedure may be employed to solve the set of equations. Upon finding  $T_{w_i}$ , the convection as well as radiation heat flux distributions,  $q_{w_i}$  and  $q_{r_i}$ , can be subsequently evaluated from equations (10) and (11), respectively.

### Fluid-Solid Coupling

The fluid and solid-side models of the previous sections are iteratively solved to obtain unique solutions to a conjugate problem. The computations proceed as follows. It can be noted in the following computations that the values of the parameters within each element are computed based on the lumped-capacitance method, and they are assigned at the mid-location of the element.

1 The thermo-physical properties of the fluid and solid are determined at the ambient temperature, and they are assumed to be invariant of temperature changes. An investigation of Sparrow and Gregg (1958) on the effect of variable fluid properties in natural convection indicates that the assumption of constant properties should not affect the final temperature excess by more than 2 to 3 percent over the temperature ranges that are expected to occur in the problems of the current interest.

2 The plate is discretized into  $N$  equal size elements. The locations of the heated elements are identified and the magnitude of their power levels are assigned.

3 To initialize the iteration procedure, any form of a positive surface heat flux variation may be used for  $q_{w_i}$ . A uniform heat flux over the entire surface of the plate is chosen whose integrated heat dissipation is identical to the sum of heat delivered by all the sources on the plate.

4 The fluid-side model is solved which results in a surface temperature variation,  $T_{w_i}$ , corresponding to the specified distribution for the convective heat flux,  $q_{w_i}$ .

5 Using the surface temperature variation obtained from the fluid-side model in step 4, the convection heat transfer coefficient,  $h_i$ , is determined from a rearranged form of equation (10) as

$$h_i = \frac{q_{w_i}}{T_{w_i} - T_f} \quad (12)$$

and the radiative heat flux,  $q_{r_i}$ , is computed by means of the Stefan-Boltzmann law of thermal radiation, equation (11).

6 Using  $h_i$  and  $q_{r,i}$  from the above, the solid-side model is solved for a new surface temperature distribution,  $T_{w,i}$ . An improved prediction of  $q_{r,i}$  can then be computed based on the new  $T_{w,i}$ , and this computation can be taken iteratively in order to improve the solutions. But, an excessive convergence is found unnecessary at this step since the  $h_i$  values from equation (12) will be modified again by the fluid-side model in the next outer iteration. Approximately 3 to 5 iterations of this step were found to be sufficient.

7 The temperature distribution obtained from the solid-side model in the above step is compared with that obtained from the fluid-side model in step 4. If these two temperature distributions agree to within a specified tolerance, the arithmetic average of the two distributions is used as the "converged" surface temperature solution to the conjugate problem. Otherwise, the convection heat flux distribution,  $q_{w,i}$ , is re-evaluated using  $h_i$  from equation (12) and  $T_{w,i}$  from step 6, and steps 4 to 7 are repeated.

## Results and Discussions

Computations are carried out following the procedures described in the previous section for two dimensional cases of a vertical plate. The plate has two identical strip heat sources and is cooled by natural convection in air. A dimensional configuration of the plate is given in Fig. 4, where thickness of the plate is shown greatly exaggerated and hatched surfaces indicate those that are insulated. The variables used in the computations are as follows:

Input heat flux:

$$q_p = 3875 \text{ W/m}^2$$

$$l = 0.508 \times 10^{-2} \text{ m}$$

Solid:

$$L = 9.652 \times 10^{-2} \text{ m}$$

$$t = 1.143 \times 10^{-3} \text{ m}$$

$$k_s = \begin{cases} 1.032 \text{ W/mK} & \text{for glass plate} \\ 28.38 \text{ W/mK} & \text{for ceramic plate} \end{cases}$$

$$\epsilon = \begin{cases} 0.387 & \text{with glass plate} \\ 0.366 & \text{with ceramic plate} \end{cases}$$

Fluid (air):

$$T_f = 298 \text{ K}$$

$$\nu = 15.614 \times 10^{-6} \text{ m}^2/\text{s}$$

$$k_f = 0.0258 \text{ W/mK}$$

$$\text{Pr} = 0.72$$

Surroundings:

$$T_\infty = 298 \text{ K}$$

As shown above, two different values are used for the plate properties in order to simulate the glass and ceramic plates as they were employed by Zinnes (1969) in his numerical and experimental investigation.

All computations in the present study were performed using an IBM AT personal computer. A tolerance of  $0.4^\circ\text{C}$  was used as the convergence criterion upon the surface temperature variations, so that the resulting solution would be within  $0.2^\circ\text{C}$  from either the fluid or the solid-side temperature

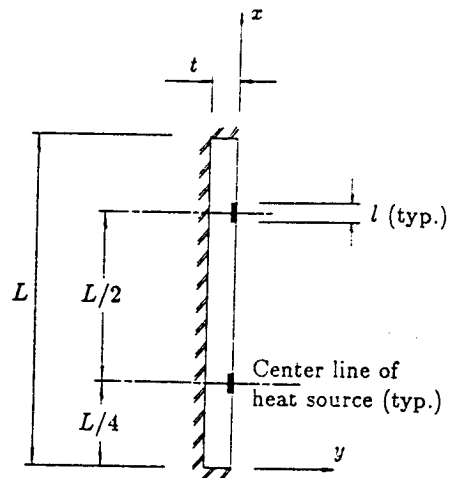


Fig. 4 Geometric configuration of test plate

distribution at any locations on the plate surface. The maximum temperature difference between the fluid and solid-side predictions always occurred in the downstream region of the last heat source before the end of the plate. The model is stable and converges fast. The typical computation was terminated after 2 to 3 iterations for the ceramic plate and 7 to 10 iterations for the glass plate. The computing time is largely dependent on the number of elements used. With efficient programming each iteration takes about 2 to 10 minutes for  $N=38$  elements. More than 90 percent of this time is consumed in solving numerically the ordinary differential equation for  $\gamma_i$  using the Runge-Kutta formula. Doubling the number of elements to 76 increased computing time by 3 to 4 times but did not noticeably improve the final results. The data plotted in this paper are those of the 76 element discretization.

The resulting surface temperature variations are compared with those obtained by Zinnes (1969) in Figs. 5 and 6 for the glass and ceramic plates, respectively. All the data of Zinnes presented in these figures, as well as in the figures to follow, have been reproduced by carefully digitizing his reported plots and transforming the variables to those shown in the figures. Also shown and compared in these figures are the surface temperature variations that would have resulted from the same plates if radiation heat transfer were excluded. Higher temperature distributions are observed over the entire plates as expected. For the glass plate, the maximum temperature is increased by as much as about  $20^\circ\text{C}$ .

An examination of Figs. 5 and 6 reveals the effect of the plate thermal conductivity on the temperature distributions. It is shown that, as the thermal conductivity of the board increases, the local maximum temperatures are reduced, and the heat transported from the sources by means of conduction raises the lower temperatures in the off-source regions. This results in smaller temperature gradients along the board and, therefore, warpage becomes less of a problem.

In anticipation of possible large temperature gradient in localized regions near the plate, Zinnes included the effect of axial conduction in the fluid in his numerical computations, instead of solving the boundary layer form of the energy equation, equation (3). Nevertheless, excellent agreement of the present model with the numerical methods is obtained validating the use of the boundary layer approximations, even for the glass plate. The thermal conductivity of the glass plate, which is about  $1 \text{ W/mK}$ , can be considered low in applications. But, since this still represents about 40 times the conductivity of air at room temperature, it would be reasonable to conclude that the in-plane conduction is predominantly characterized by the plate conductivity alone in most cases in air.

The radiation and convection heat flux distributions are

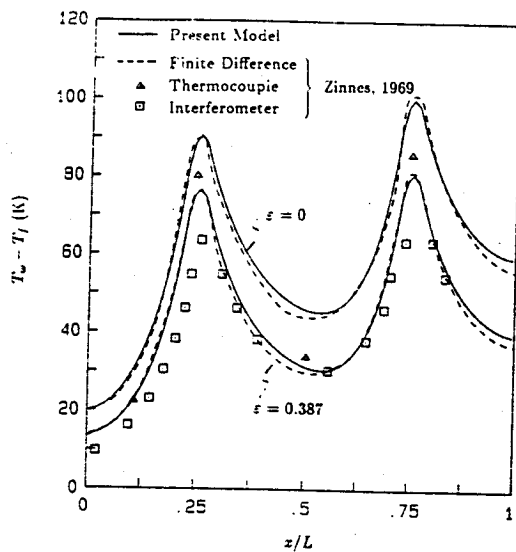


Fig. 5 Comparison of wall temperature excess of glass plate ( $k_s = 1.032$  W/mK) over ambient fluid temperature  $T_f$  at  $25^\circ\text{C}$ ; with and without radiation heat transfer

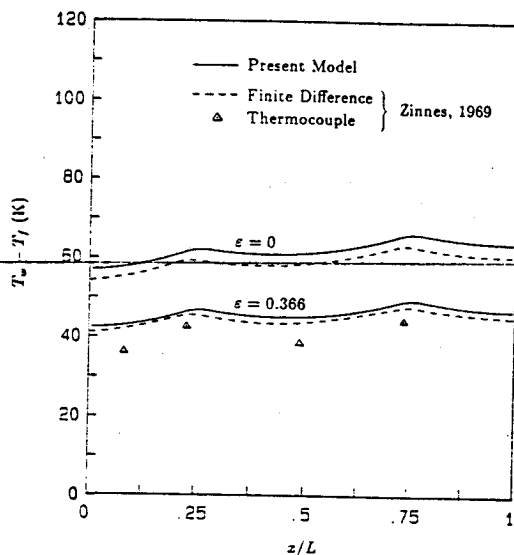


Fig. 6 Comparison of wall temperature excess of ceramic plate ( $k_s = 28.38$  W/mK) over ambient fluid temperature  $T_f$  at  $25^\circ\text{C}$ ; with and without radiation heat transfer

shown in Fig. 7 for both the glass and ceramic plates. The significance of the radiation heat transfer is once again revealed in this figure as the total radiation heat transfer, represented by the area under the curve, accounts for up to, in excess of 30 percent of the total heat dissipation in both cases.

A dimensionless convective heat flux is defined as

$$q_w^* = \frac{q_w L}{(T_w - T_f) k_f} \quad (13)$$

This equation is evaluated for the glass and ceramic plates. Results are compared again with the numerical data of Zinnes (1969) in Fig. 8. As can be seen from the figure, agreement is excellent for the case of the ceramic plate. But, somewhat poor agreement is observed for the case of the glass plate, having as much as 20 percent differences over the regions where the heat sources are located. Recalling the near perfect agreement in the surface temperature variation of the glass plate over the source regions from Fig. 5, it can be said that the poor agreement is attributed mainly to the local differences in the prediction of the convective heat flux variations over the sources between the two methods, as observed in Fig. 7.

The Biot number can be evaluated from

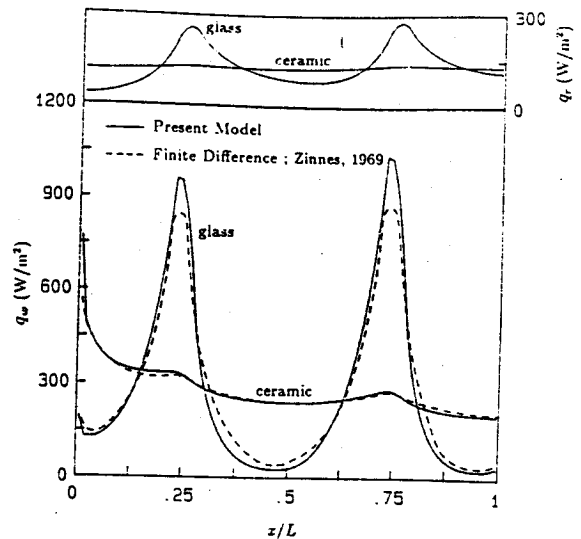


Fig. 7 Radiative heat flux and comparison of convective heat flux

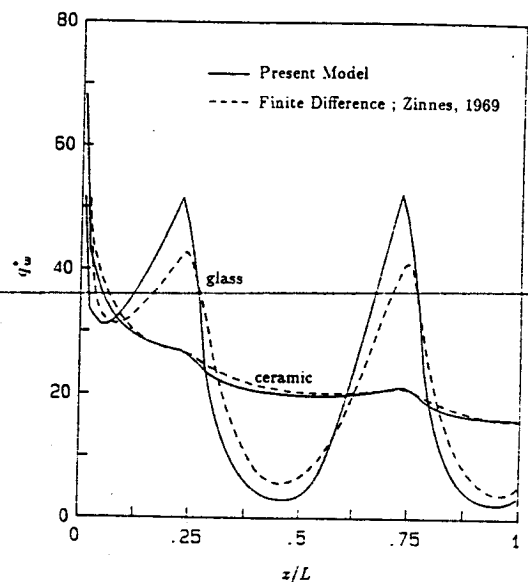


Fig. 8 Comparison of dimensionless surface heat flux

$$\text{Bi} = q_w^* \times \frac{t}{L} \times \frac{k_f}{k_s} \quad (14)$$

For the case with the glass plate, Fig. 8 shows that the maximum values of  $q_w^*$  over the sources are in the vicinity of 53. This results in Bi of 0.016, and the use of the one dimensional solid-side model is therefore justified, not only for the glass plate, but also for the ceramic plate.

The temperature and  $u$ -velocity distributions in the boundary layer are plotted in Fig. 9 for the case with the glass plate. They are computed by using the fluid-side model, and their expressions are presented in the earlier study of Lee and Yovanovich (1989). The figure shows that the velocity distribution is relatively insensitive to the changes in the upstream temperature distribution, although the fluid velocity is induced by the buoyant force which is imposed by the temperature excess in the fluid.

In addition to the cases examined herein, Zinnes also computed and tested other cases in which an additional strip heat source was mounted at the mid-length of the plate. He was able to examine a number of cases with different heating arrangements by deactivating individual sources at a time. Comparisons of the surface temperature variations obtained by using the present model for various combinations of heating ar-

